Transverse Energy Flow in Deep Inelastic Scattering

K. Wacker[a]*
representing the H1 Collaboration

[a]Institut für Physik, Universität Dortmund, D-44221 Dortmund, Germany

The transverse energy flow was measured in deep inelastic scattering by the H1 detector at HERA for $Q^2 > 2.5\,\mathrm{GeV}^2$ with x_B down to $3 \cdot 10^{-5}$. The results are compared to QCD based models.

1. INTRODUCTION

The transverse energy (E_T) flow is a variable relatively easy to measure in a calorimeter and it is sensitive to the QCD description of the deep-inelastic scattering (DIS) final state and its dependence on kinematic variables.

DIS can be viewed in two complementary ways: as a point-like hard-scattering process or as the scattering of a virtual photon γ^* on a proton with the γ^* temporarily fluctuating to a hadron. In the latter view, one naively expects a central rapidity region independent of γ^* properties (e.g., Q^2), whereas the photon fragmentation region may show such a dependence.

$\gamma^* p$ scattering is best studied in the hadronic center-of-mass system (hCMS), whereas the Breit frame is advantageous for the study of DIS as hard scattering. The transformation between the two frames is a boost along the proton beam direction with a rapidity of $1/2 \ln(1/x - 1)$.

In these proceedings only a rough description of the analysis can be given. Full details will be published [1].

2. ENERGY FLOW DETECTORS

The H1 detector has been described in detail elsewhere [2]. The main instrument to measure energy flow in H1 is the Liquid Argon Calorimeter (LAr). It covers the angular range $4^\circ < \Theta < 154^\circ$ with $\geq 4\lambda_I$ with high segmentation. The backward area (roughly $155^\circ < \Theta < 176^\circ$) is covered by an electromagnetic calorimeter. Until 1994, this was the Backward Electromagnetic Calorimeter (BEMC), which had only $\approx 1\lambda_I$. It was then replaced with the SpaCal, which has $\approx 2\lambda_I$.

The extreme forward area is covered by the Plug calorimeter. There is unfortunately a large and variable amount of passive material (0.8 to $5\lambda_I$) in front of it, which leads to losses and scattering into different angular regions. This has to be corrected for by simulation.

3. THE EVENT SAMPLES

The Q^2 range below $100\,\mathrm{GeV}^2$ was investigated with 1994 data where the scattered electron was detected in the BEMC. The $2.7\,\mathrm{pb}^{-1}$ data sample with nominal vertex was augmented by a $0.058\,\mathrm{pb}^{-1}$ sample with shifted vertex position, which allowed to go to a lower Q^2 limit of $2.5\,\mathrm{GeV}^2$.

For the Q^2 range above $100\,\mathrm{GeV}^2$, 1996 data with $8.2\,\mathrm{pb}^{-1}$ were used with the scattered electron detected in the LAr.

Events were required to have an identified electron with an energy $E_e > 12\,\mathrm{GeV}$ and a reconstructed vertex. The scaling variable y was required to be in the range $0.05 \lesssim y < 0.6$. Further cuts were made to reduce the number of radiative events using the longitudinal momentum balance and a comparison of the kinematic variables x, y and Q^2, which in this analyses are calculated using the parameters of the scattered electrons, with the values obtained with other methods. Furthermore, cuts against events with a rapidity gap near the proton beam direction were

*Supported by the Bundesministerium für Bildung, Wissenschaft, Forschung und Technologie under contract number 7DO55P

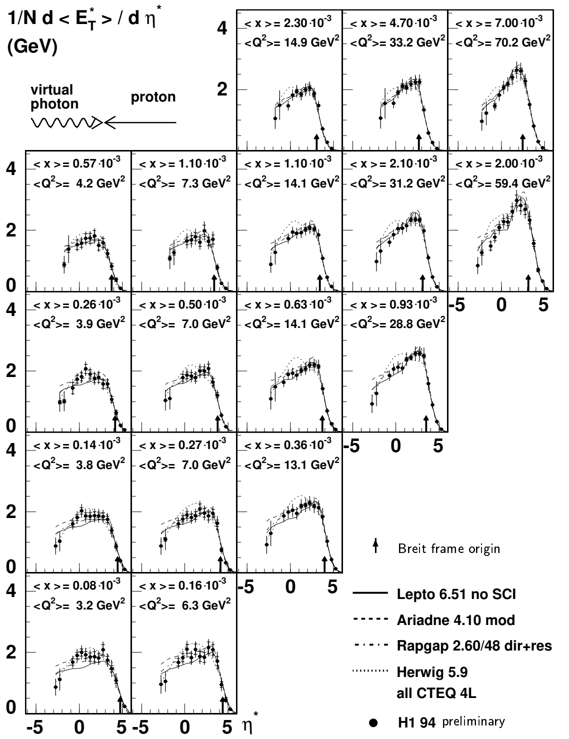

Figure 1. The inclusive transverse energy flow at different values of x and Q^2 for the low Q^2 sample.

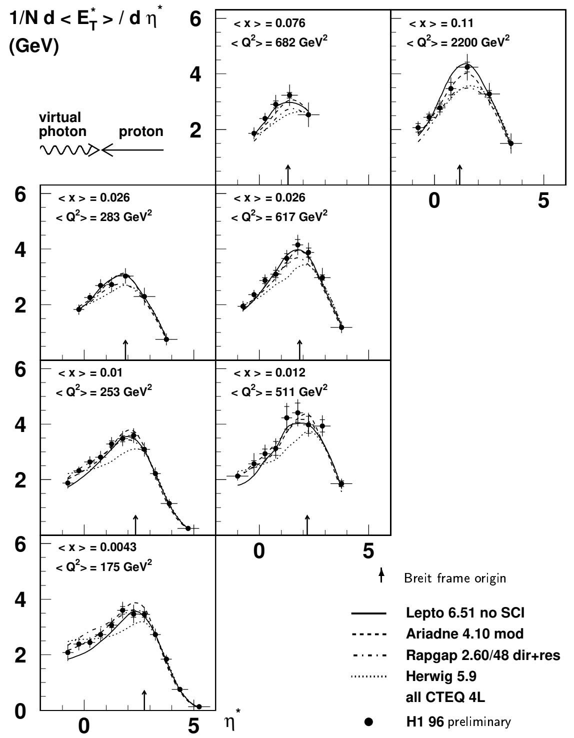

Figure 2. The inclusive transverse energy flow at different values of x and Q^2 for the high Q^2 sample.

made.

4. EXPERIMENTAL METHOD

The quantity of interest is the transverse energy $E_T^* = E^* \sin\Theta^*$ in the hCMS. In the laboratory system there is a "trivial" kinematical contribution to $E_T \propto Q$. The Lorentz transformation has to be known precisely to remove this contribution. Radiative events (see above) and the energy measurement of the scattered electron are the most problematic points. These effects influence mostly the component of E_T in the event plane. It is thus advantageous to use $E_\perp^* = E_T^* |\sin\phi^*| \frac{\pi}{2}$ instead of E_T^*, where ϕ^* is the azimuthal angle w.r.t. the event plane. Note that $\langle E_\perp^* \rangle = \langle E_T^* \rangle$.

Bin-by-bin corrections were made to account for radiative and detector effects using the DJANGO event generator and the H1 detector simulation program.

Systematic errors were evaluated in detail. The most direct systematic error comes from hadronic energy scale uncertainties of the calorimeters. The systematic errors add up to 7% – 22% (35% in the PLUG region).

5. QCD PREDICTIONS

To arrive at QCD predictions, the DIS reaction has to be modeled in steps. The parton (or partons in case of a hadron-like photon) which undergo hard scattering emerge from the beam particles according to a parton distribution function. We use the CTEQ 4L [3] set for the proton and the SAS-G [4] description of the virtual pho-

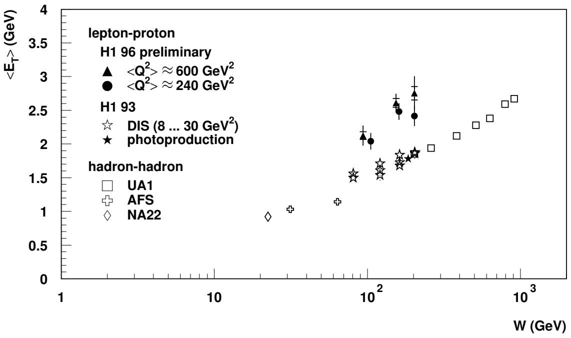

Figure 3. W-dependence of $\langle E_T^* \rangle$.

ton. The partons involved in the hard scattering may undergo further QCD evolution which is modeled in different ways. The outgoing partons finally hadronise according to the string model [5] as implemented in JETSET 7.4 [6] in all QCD predictions considered here. The settings of parameters in the QCD models were adjusted by their authors after these data were first presented [7]. Details are described in Ref. [1].

6. RESULTS

Fig. 1 shows the transverse energy flow as a function of the pseudo-rapidity η^* in the hCMS for the low Q^2 sample, Fig. 2 shows the same for the high Q^2 sample. At low x and Q^2 we observe a flat distribution at the level of $\approx 2\,\mathrm{GeV}$. $\langle E_T^* \rangle$ rises with increasing Q^2, particularly in the photon fragmentation region. At the highest Q^2, it develops a maximum near the origin of the Breit frame.

The QCD model calculations shown in the figures reproduce the general shape of the data. There are discrepancies in detail: LEPTO is below the data points in the central region at low x and Q^2. HERWIG shows a peak at $\eta^* \approx 1$ which is not in the data. RAPGAP and HERWIG are unable to describe the data at the highest Q^2 values. ARIADNE shows very high $\langle E_T^* \rangle$ values in the proton fragmentation region.

Fig. 3 shows the W dependence of $\langle E_T^* \rangle$ for two

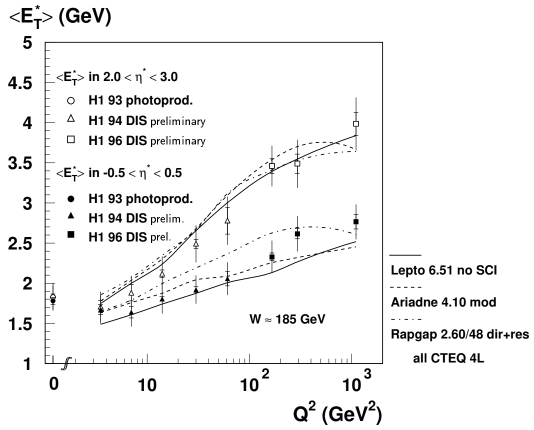

Figure 4. $\langle E_T^* \rangle$ as function of Q^2 in two η^* regions in a narrow W range of $165\,\mathrm{GeV} < W < 213\,\mathrm{GeV}$

high-Q^2 regions. Also shown are earlier H1 results for low-Q^2 DIS and photoproduction [9] and results from hadron-hadron collisions [10]. We find higher values of $\langle E_T^* \rangle$ than at low Q^2 and in hadronic reactions, but the W-dependence is similar.

In order to study the Q^2 dependence of $\langle E_T^* \rangle$, we plot the $\langle E_T^* \rangle$ spectra as function of η^* in different Q^2 bins in a narrow W range of $165\,\mathrm{GeV} < W < 213\,\mathrm{GeV}$. We select an η^* range representing the central region ($-0.5 < \eta^* < 0.5$) and another one for the photon fragmentation region ($2 < \eta^* < 3$). Fig. 4 shows the resulting Q^2 dependence of $\langle E_T^* \rangle$. We see that $\langle E_T^* \rangle$ rises strongly with Q^2 in the photon fragmentation region and less strong, but still significant, in the central region.

7. CONCLUSIONS

The transverse energy flow was measured in DIS for $Q^2 > 2.5\,\mathrm{GeV}^2$ with x_B down to $3 \cdot 10^{-5}$. The E_T-flow as function of η^* develops a peak approximately at the origin of the Breit frame with rising Q^2. There is an increase of $\langle E_T^* \rangle$ also in the central rapidity region which is not expected in a simple picture of a photon fluctuating into a hadron. QCD-based models give an acceptable overall description, but all models have difficulties describing the data in detail.

REFERENCES

1. H1 Collaboration, paper in preparation.
2. H1 Collaboration, I. Abt et al., NIM **A386** (1997) 310; H1 Collaboration, I. Abt et al., NIM **A386** (1997) 348.
3. CTEQ Collaboration, MSUHEP-60426, CTEQ-604.
4. G. Schuler and T. Sjöstrand, Phys. Lett. **B376** (1996) 193.
5. B. Andersson, G. Gustafson, G. Ingelman and T. Sjöstrand, Phys. Rep. **97** (1983) 31.
6. T. Sjöstrand, Comp. Phys. Comm. **82** (1994) 74.
7. D. Krücker in Proc. of the 6th International Workshop on DIS and QCD, Brussels 1998.
8. L. Lönnblad, Comp. Phys. Comm. **71** (1992) 15.
9. H1 Collaboration, S. Aid et al., Phys. Lett. **B358** (1995) 412.
10. UA1 Collaboration, C. Albajar et al., Nucl. Phys. **B335** (1990) 261; A. De Roeck, Ph.D. Thesis, Antwerpen 1988.